Silsesquioxane-Cross-Linked Porous Nanocomposites Synthesized within High Internal Phase Emulsions

Jenny Normatov and Michael S. Silverstein*

Department of Materials Engineering, Technion-Israel Institute of Technology, Haifa 32000, Israel

Received June 26, 2007; Revised Manuscript Received September 5, 2007

ABSTRACT: Novel silsesquioxane-cross-linked porous nanocomposites with densities of around 1.5×10^2 kg/m^3 were synthesized within high internal phase emulsions (HIPE) in which 2-ethylhexyl acrylate (EHA) was cross-linked and reinforced with vinyl silsesquioxane (VSQ). The molecular structure, porous structure, thermal properties, mechanical properties, and pyrolysis were investigated. The tan δ peak temperature, tan δ full width at half-maximum, room-temperature modulus, and stress at 40% strain all increased in a linear fashion with increasing VSQ content, reflecting the increase in cross-linking through reaction with the reinforcing Si−O network. The VSQ-containing polyHIPE were compared to polyHIPE based on EHA cross-linked with divinylbenzene (DVB) and reinforced by reaction with a polyhedral oligomeric silsesquioxane (POSS) bearing one vinyl group. On a molar basis, cross-linking with DVB produced higher tan δ peak temperatures and moduli, and this was related to the presence of unreacted VSQ vinyl groups. However, the POSS-containing polyHIPE had significantly higher tan δ peak temperatures and moduli for similar Si contents. Porous inorganic monoliths were produced on pyrolysis of these VSQ-containing polyHIPE.

Introduction

A high internal phase emulsion (HIPE) has been defined as an emulsion in which the internal phase occupies more than 74% of the volume, corresponding to the maximum packing fraction of monodispersed droplets. PolyHIPE are porous cross-linked polymers based on HIPE and result from polymerization of monomers and cross-linking comonomers in the HIPE's continuous phase.[1,2] The changes in density and surface tension during polymerization lead to the development of holes within the thin layer of continuous phase separating the discrete droplets. These holes connect the droplets and produce a bicontinuous phase structure.[3] Cross-linking is necessary for polyHIPE stability, and a cross-linking comonomer is used. The amount of cross-linking comonomer needed to stabilize polyHIPE is often quite substantial. If the extent of cross-linking is not high enough then the polyHIPE will either collapse into a dense material or disintegrate into a powder during polymerization and/or drying. A wide variety of monomers and cross-linking comonomers have been used for polyHIPE synthesis.[1,2,4,5] In addition, interpenetrating polymer networks (IPN) polyHIPE, polyHIPE with intrinsically conductive polymers, crystallizable polyHIPE, hybrid polyHIPE, hydrogel polyHIPE, and polyHIPE containing inorganic fillers have been synthesized.[6−19]

Porous materials have numerous applications in such areas as catalysis, chromatography, and separation, where control over pore structure and pore size strongly influences the efficiency of the material.[20] PolyHIPE, with their high porosities, high degrees of interconnectivity, and unique micrometer- to nanometer-scale open-pore structures, have been investigated for applications such as filtration media, supports for heterogenic catalytic reactions, absorbents, ion-exchange systems, and heat-resistant structural foams.[1,2,21−27] Formation of a nanocomposite polyHIPE could yield superior thermal and mechanical properties.

Polymer nanocomposites have been used to enhance the mechanical properties and thermal stabilities of polymers. Silsesquioxanes (SSQ), with the empirical formula $RSiO_{1.5}$, include random structures, ladder structures, cage structures, and networks.[28] Modification of polymers with SSQ has been used to enhance such properties as use temperature, oxidation resistance, surface hardening, mechanical properties, and flammability resistance.[29−32] Methyl silsesquioxane (MSQ) and vinyl silsesquioxane (VSQ) have pre-existing network structures that include cage-like structures, as seen in Figure 1 for VSQ. The pre-existing network structures in MSQ and VSQ can be extended through curing, condensation of the Si−OH groups seen in Figure 1.[33] MSQ has been investigated as a potential low dielectric constant (low-*k*) material for upcoming generations of integrated circuits.[28,34,35] MSQ has also been extensively investigated as a nanometer-scale filler for polymer nanocomposites.[28,36]

There are several routes available for incorporating SSQ into a polyHIPE and forming a nanocomposite. One route would be to add trialkoxysilanes to the monomers in the HIPE and form an SSQ network through alkoxysilane hydrolysis and condensation (HC) reactions. The extent of the Si−O network would depend on the synthesis conditions. Adding a trialkoxysilane that does not react with the monomers would yield an SSQ network that is not chemically attached to the polymer network. Adding a trialkoxysilane that does react with the monomers would yield an SSQ network that is covalently attached to the polymer backbone.[7,37−39] A second route for SSQ incorporation would be to add a pre-existing SSQ structure to the monomers. Such structures would include networks (such as MSQ and VSQ) and polyhedral oligomeric silsesquioxane (POSS) cages. If the SSQ does not react with the monomers (e.g., MSQ) then a blend is formed. If the SSQ can only react once with the monomers (e.g., POSS cages bearing only one vinyl group) then the SSQ is grafted to the polymer backbone.[40] If the SSQ can react multiple times with the monomers (e.g., VSQ) then the SSQ cross-links the polymer.

This manuscript describes the synthesis of novel nanocomposite polyHIPE based on 2-ethylhexyl acrylate (EHA) with VSQ as a nanoscale cross-linking reinforcement. EHA was

* To whom correspondence should be addressed. E-mail: michaels@tx.technion.ac.il.

10.1021/ma071417t CCC: $37.00
Published on Web 10/19/2007

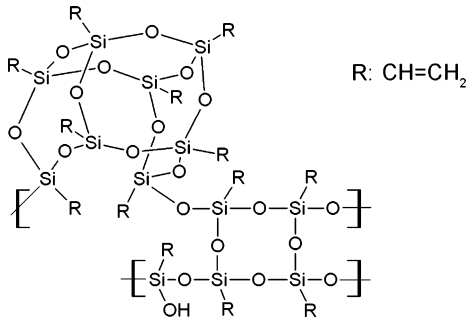

Figure 1. Structure of vinyl silsesquioxane.

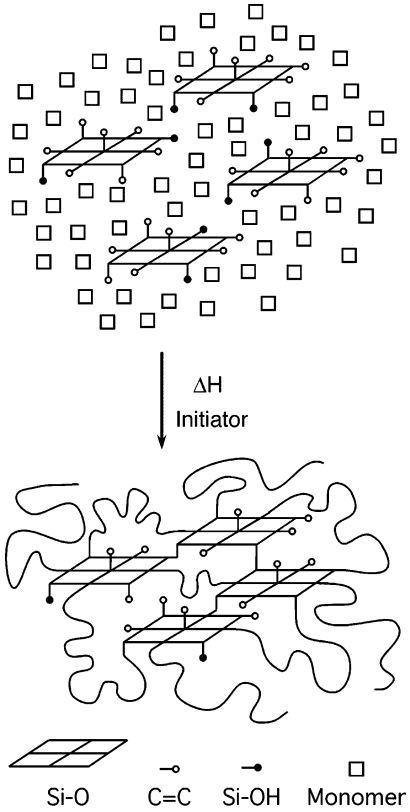

Figure 2. Schematic illustration of nanocomposite polyHIPE formed by vinyl free-radical reactions and SiOH condensation reactions.

chosen since PEHA has a glass-transition temperature (T_g) of −50 °C and is often used as a cross-linked and reinforced elastomer. EHA-based polyHIPE are flexible and can undergo relatively large deformations reversibly without failure.[6] As a rule, polyHIPE are cross-linked using organic comonomers. The nanocomposite polyHIPE described here are unique in that they are cross-linked through reaction with a pre-existing SSQ network, as illustrated schematically in Figure 2. The combination of vinyl free-radical reactions (EHA and VSQ) and Si−OH condensation reactions (VSQ) can be used to produce a stable polyHIPE that is reinforced on the nanometer scale. Introduction of a cross-linking reinforcement at the nanoscale is expected to have a significant effect on segmental mobility.

Experimental Section

Materials. The monomer used for polyHIPE synthesis was EHA (Aldrich). The emulsifier was sorbitan monooleate (SMO, Span 80, Fluka Chemie). The water-soluble initiator was potassium persulfate ($K_2S_2O_8$, Riedel-de-Haen). The HIPE stabilizer was potassium sulfate (K_2SO_4, Frutarom, Israel). The reinforcing cross-linker was VSQ with a density of 1.2×10^3 kg/m^3 (Hybrid Plastics). The basic structural unit of VSQ, used to calculate representative molar quantities, was $CH_2{=}CH{-}SiO_{1.5}$. The polyHIPE cross-linked with VSQ can be compared to polyHIPE cross-linked with divinylbenzene (DVB, which contains 40% ethylstyrene, Riedel-de-Haen) using a EHA/DVB molar ratio of 74/26 and containing 0−9 mol % POSS.[40] The POSS used to reinforce these polyHIPE was propylmethacrylcyclohexyl-POSS ($(C_6H_{11})_7Si_8O_{12}C_7H_{11}O_2$, Hybrid Plastics), which contains one vinyl group per POSS cage. EHA and DVB were washed to remove the inhibitor (once with an aqueous solution of 5 wt % sodium hydroxide (NaOH) and then three times with deionized water).

Table 1. HIPE Compositions and PolyHIPE Densities

PolyHIPE	EHA/DVB/VSQ, wt %	EHA/DVB/VSQ, mol %	Si, atom %	ρ, kg/m^3
D-26	80/20/0	74/26/0	0.0	1.3×10^2
V-40	78/0/22	60/0/40	4.1	1.6×10^2
V-50	70/0/30	50/0/50	5.7	1.4×10^2
V-61	60/0/40	39/0/61	7.8	1.5×10^2

Table 2. Typical PolyHIPE Recipe (V-40)

	component	amount, wt %
organic phase	EHA	7.77
	VSQ	2.19
	SMO	1.94
	total	11.90
aqueous phase	H_2O	87.42
	$K_2S_2O_8$	0.19
	K_2SO_4	0.49
	total	88.10

PolyHIPE Synthesis. The organic phase of the HIPE consisted of EHA, VSQ, and emulsifier. The EHA/VSQ molar ratio was varied from 60/40 to 39/61 (Table 1). The polyHIPE nanocomposites are named V-*x*, where *x* indicates the molar percentage of VSQ in the EHA/VSQ mixture. The aqueous phase consisted of deionized water containing initiator and stabilizer (K_2SO_4 and $K_2S_2O_8$, respectively). The mass ratio of organic phase to aqueous phase was held at approximately 1:9. The recipe for a typical sample (V-40) is given in Table 2. The organic phase of the polyHIPE used for comparison contained EHA, DVB, POSS, and emulsifier. The reference EHA/DVB polyHIPE (no POSS) will be referred to as D-26 (Table 1).

The polyHIPE synthesis procedure was described in detail elsewhere and is unchanged for the synthesis of the nanocomposite polyHIPE.[6] Briefly, the aqueous phase was added slowly to the organic phase with continuous stirring. Polymerization took place in a convection oven at 65 °C for 24 h. The polyHIPE was dried in a vacuum oven at 60 °C for about 48 h. The emulsifier, initiator, and stabilizer were removed by Soxhlet extraction in deionized water for 24 h and methanol for 24 h. The polyHIPE was then dried in a convection oven at 60 °C for 12 h.

Characterization. The densities of the polyHIPE were determined from gravimetric analysis. The molecular structures were characterized using photoacoustic Fourier transform infrared spectroscopy (PA-FTIR, Bruker) and X-ray photoelectron spectroscopy (XPS) (Thermo Sigma Probe, VG Scientific). The porous structure was characterized using high-resolution scanning electron microscopy with uncoated specimens and accelerating voltages of 2.5−5 kV (HRSEM, LEO 982, Zeiss). The thermal properties were characterized using dynamic mechanical thermal analysis (DMTA) temperature sweeps at 3 °C/min at a frequency of 1 Hz on $7 \times 7 \times 7$ mm^3 cubes in compression (MK III DMTA, Rheometrics). The mechanical properties were characterized using compressive stress−strain measurements on $5 \times 5 \times 5$ mm^3 cubes at 25 °C (MK III DMTA, Rheometrics). The measurements were carried out until an equipment-related force limitation was reached. The modulus, *E*, was calculated from the slope of the stress−strain curve at low strains. Thermogravimetric analysis (TGA) was conducted in air from 25 to 1000 °C at 20 °C/min (2050 TGA, TA Instruments). The differential thermogravimetry (DTG) curves,

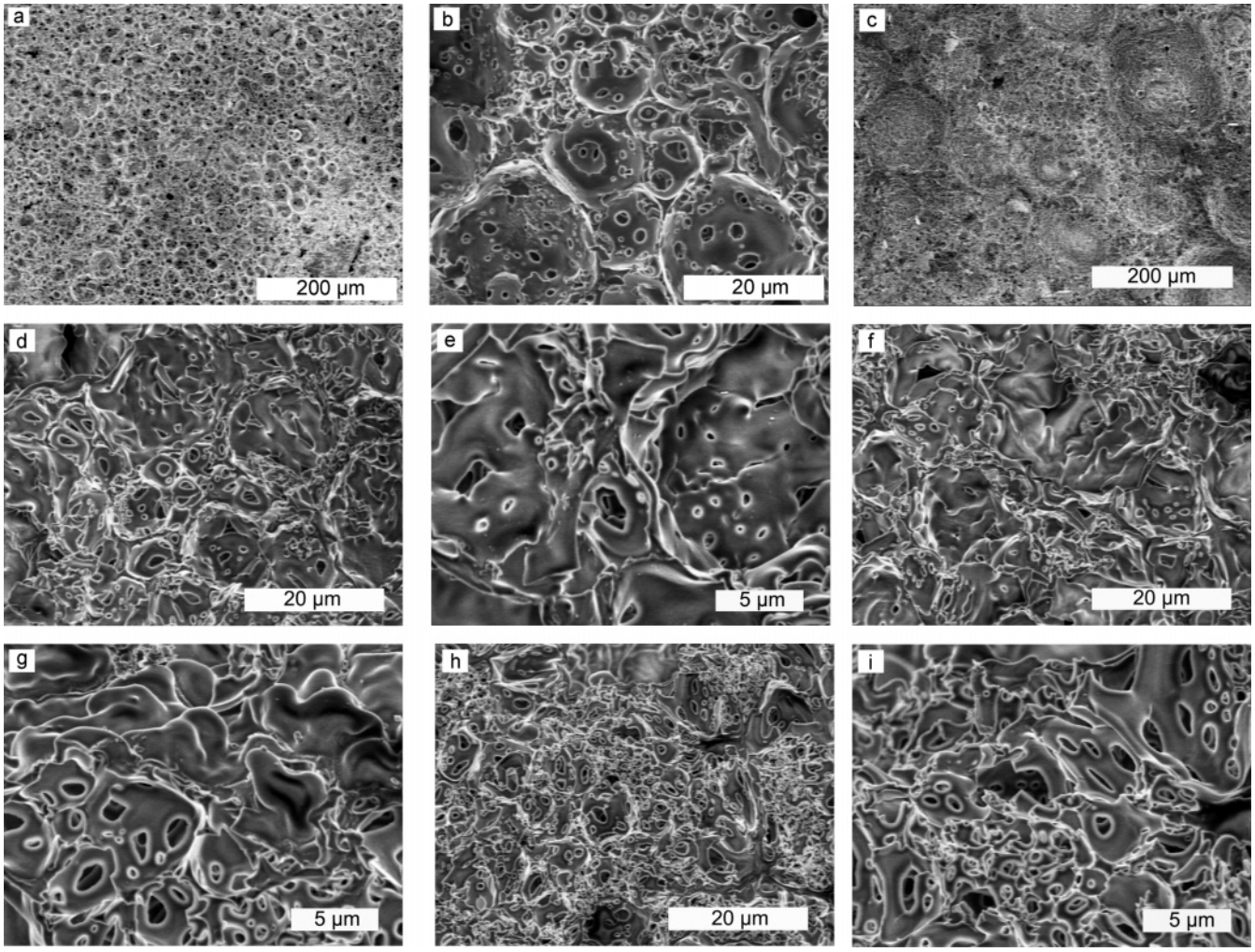

Figure 3. SEM micrographs of D-26 and nanocomposite polyHIPE: (a and b) D-26, (c−e) V-40, (f and g) V-50, and (h and i) V-61.

derivatives of the TGA thermograms, were calculated using the supplied software.

Results and Discussion

PolyHIPE Structure. The HIPE with VSQ contents above 40 mol % yielded polyHIPE with minimal shrinkage. The densities of the nanocomposite polyHIPE are around 1.5×10^2 kg/m^3. The density of D-26 is 1.3×10^2 kg/m^3, and the porosity, estimated by assuming a polymer density of 1.1×10^3 kg/m^3, is around 88% (Table 1). The slightly higher densities for the nanocomposite polyHIPE indicate that the porosities are somewhat less than that of D-26. A HIPE with a VSQ content of 21 mol % (10 wt %) shrank to about one-half its volume during polymerization, yielding a tacky polymer. The cross-link density and stiffness provided by 21 mol % VSQ were insufficient to provide the stability needed to prevent the collapse of the EHA-based polyHIPE. Similar results were observed for EHA-based polyHIPE that had less than 26 mol % DVB.[6] A VSQ content of 40 mol % was needed to provide polyHIPE stability through a combination of increasing the cross-link density and increasing the T_g.

The porous structure typically found in polyHIPE from relatively stable HIPE consists of 'voids', the volume vacated by the droplets of the dispersed phase, and 'holes', the openings in the wall structure that surrounds the voids. This combination of voids and holes creates the open-pore structure seen for D-26 in Figure 3a,b. The structures in Figure 3c−i indicate that the HIPE/polyHIPE that contain VSQ underwent destabilization. The destabilization increased with increasing VSQ content and can be related to changes in the HIPE interfacial tension.[5] Addition of tetraethylorthosilicate (TEOS) to an EHA-based polyHIPE had a similar destabilizing effect.[16] V-40, in Figure 3c, exhibits large spherical and spheroidal voids on the order of 50−100 μm that result from this destabilization.[41,42] There are, in addition, voids on the order of 5−15 μm that are typical of polyHIPE structures (Figure 3d,e). The voids are connected by holes of around 0.5−2 μm in diameter. V-50 and V-61 exhibit porous structures (Figure 3f,g and 3h,i, respectively), but it is much more difficult to discern a typical polyHIPE structure in these materials. HIPE/polyHIPE destabilization seems more extensive at higher VSQ contents. In spite of this destabilization, V-50 and V-61 are highly porous.

The FTIR spectra from the nanocomposite polyHIPE are seen in Figure 4, and selected bands are listed in Table 3.[43] The wide peak between 1000 and 1200 cm^{-1} includes the C−O band (1170 cm^{-1}) from EHA as well as the cage (1110 cm^{-1}) and network (1030 cm^{-1}) Si−O bands from VSQ.[33,44] The band at 768 cm^{-1} is associated with unreacted Si−CH=CH$_2$ groups from VSQ, and the band at 1602 cm^{-1} is also associated with unreacted vinyl groups. The FTIR spectrum from D-26 (not shown) exhibits no trace of unreacted vinyl groups at 1602 cm^{-1}.[5,40] The unreacted vinyl groups in the VSQ-containing polyHIPE, therefore, most likely originate in the VSQ. The variation with VSQ content of the normalized intensities of the bands at 768 and 1602 cm^{-1} are seen in Figure 5 (the intensities

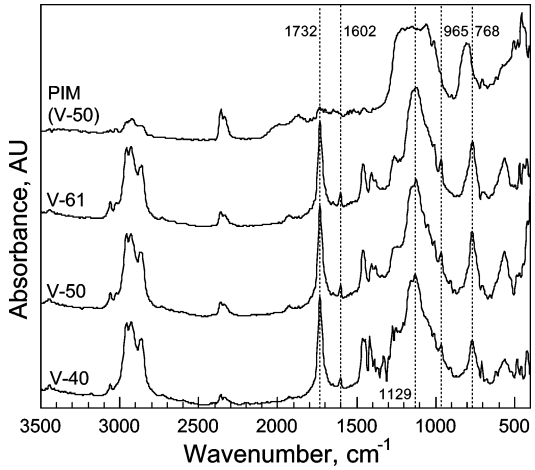

Figure 4. FTIR spectra from the nanocomposite polyHIPE and the PIM based on V-50.

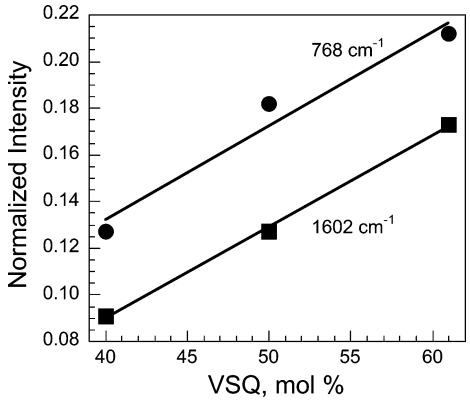

Figure 5. Variation with VSQ content of the normalized intensities of the FTIR bands at 768 and 1602 cm^{-1} (the intensities were normalized by the intensity of the ester band at 1732 cm^{-1}).

Table 3. Selected FTIR Bands and Their Assignments

band, cm^{-1}	group	comments
1732	C═O	EHA
1602	C═C	VSQ
1170	C−O	EHA
1050−1110	Si−O	VSQ
768	Si−CH═CH_2	VSQ

were normalized by the intensity of the EHA-associated ester band at 1732 cm^{-1}). The normalized intensities of these bands increase with increasing VSQ content in a linear fashion.

PolyHIPE Properties. The variation of tan δ with temperature for these nanocomposite polyHIPE is seen in Figure 6. The tan δ peak temperature and full width at half-maximum (fwhm) both increase with increasing VSQ content, and the tan δ peak height decreases with increasing VSQ content. Previous work has shown that there are two factors that produce increases in the tan δ peak temperature and fwhm and that produce a reduction in the tan δ peak height. One factor is an increase in the cross-link density, and the other factor is an increase in the amount of inorganic reinforcement.[5,16,37,40] For these nanocomposite polyHIPE, increasing the VSQ content produces both an increase in the amount of cross-linking and an increase in the amount of inorganic reinforcement. The tan δ peak temperature increases with the VSQ content (from −20 to 5 °C) in a linear fashion (Figure 7). The fwhm also increases with the VSQ content (from 49 to 66 °C) in a linear fashion (Figure 7). These changes in the tan δ peak reflect the restrictions on the segmental mobility that are imposed both by cross-linking and by grafting

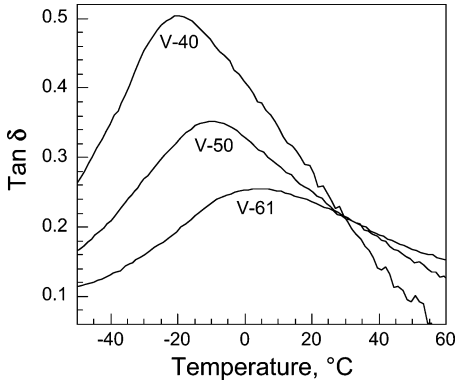

Figure 6. Variation of tan δ with temperature for the nanocomposite polyHIPE.

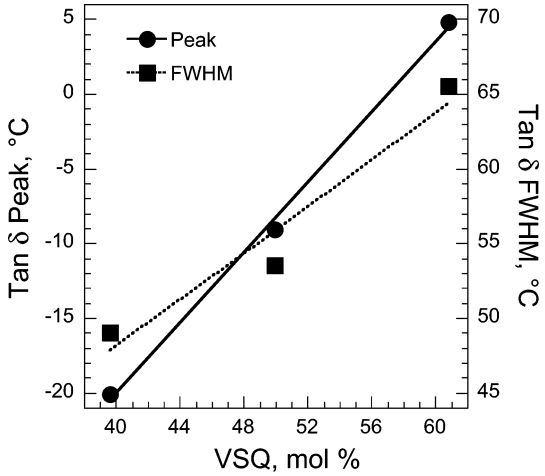

Figure 7. Variation of tan δ peak temperature and fwhm with VSQ content.

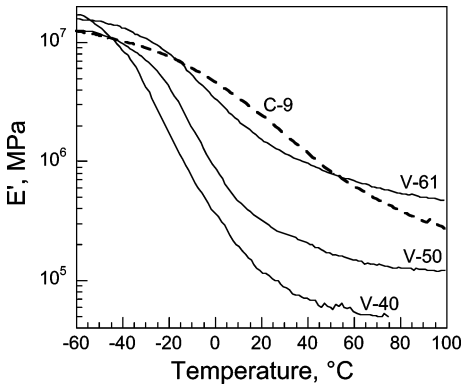

Figure 8. Variation of E' with temperature for the nanocomposite polyHIPE.

to a rigid nanometer-scale reinforcement.

The variation of E' with temperature for the VSQ-containing nanocomposite polyHIPE is seen in Figure 8. Below the T_gs the polymers are glassy and exhibit similar E' plateaus. There are, however, significant differences in the E' rubbery plateaus above the T_gs. The E' rubbery plateau for V-61 is nearly an order of magnitude greater than that for V-40. This significant increase in the E' rubbery plateau results from the increases in cross-link density and reinforcement. Both the increase in cross-link density and the increase in grafting to a rigid nanoscale reinforcement enhance molecular stiffness and yield the increase in modulus.

Room-temperature compressive stress−strain curves for the nanocomposite polyHIPE are seen in Figure 9. The stress−strain

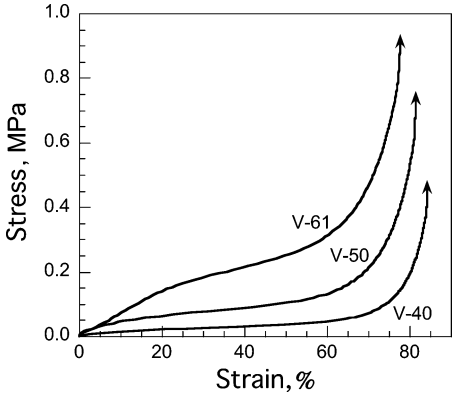

Figure 9. Compressive stress−strain curves for the nanocomposite polyHIPE.

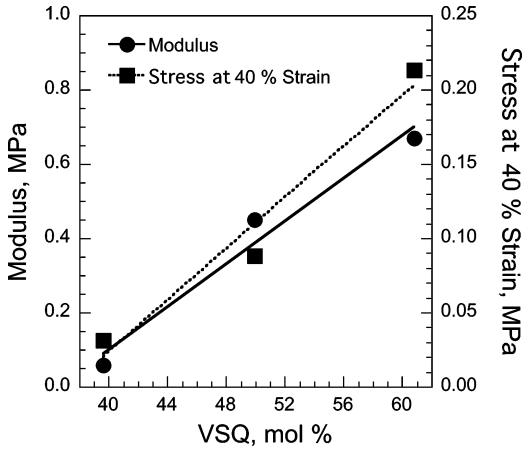

Figure 10. Variation of modulus and stress at a strain of 40% with VSQ content.

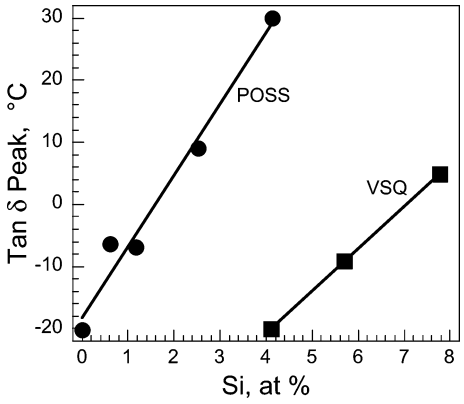

Figure 11. Variation of tan δ peak temperature with Si content for VSQ-containing and POSS-containing nanocomposite polyHIPE.

curves are typical of polyHIPE: a linear region at low strains, a stress plateau region, and a densification region with a steep increase in stress. Both the modulus and the stress of the plateau increase with increasing VSQ content. The length of the stress plateau (its strain range) and the strain at which densification begins both decrease with increasing VSQ content. The modulus increases in a linear fashion with VSQ content (Figure 10). The relatively low modulus of V-40, 0.06 MPa, reflects a relatively low degree of cross-linking/reinforcement. The increase in modulus with VSQ content (Figure 10) reflects the increase in cross-linking through reaction with the reinforcing Si−O network per mole EHA. The modulus of 0.66 MPa for V-61, an increase of over an order of magnitude, reflects a relatively high degree of cross-linking/reinforcement. The stress plateaus

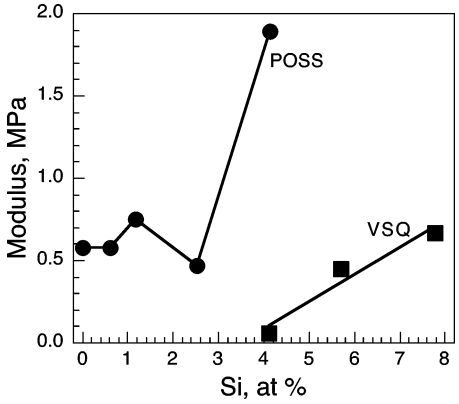

Figure 12. Variation of modulus with Si content for VSQ-containing and POSS-containing nanocomposite polyHIPE.

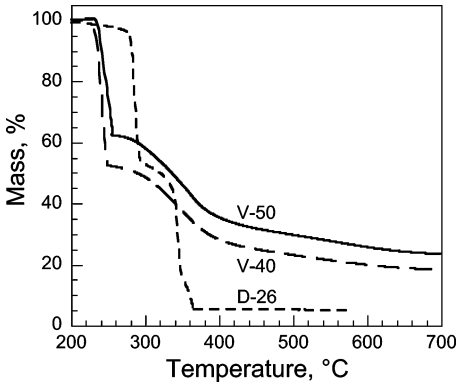

Figure 13. TGA thermograms from D-26 and the nanocomposite polyHIPE.

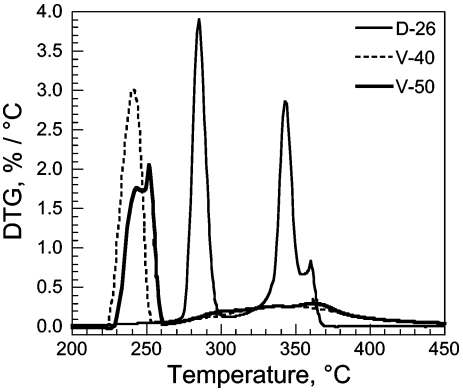

Figure 14. DTG thermograms from D-26 and the nanocomposite polyHIPE.

can be compared at a particular strain which is within the plateau region for all the polyHIPE. The stress at a strain of 40% increases with VSQ content in a linear fashion (Figure 10).

VSQ-Containing PolyHIPE versus POSS-Containing PolyHIPE. The VSQ-containing polyHIPE can be compared to the POSS-containing, DVB cross-linked, polyHIPE on the basis of the silicon content in the monomer feed. The atomic fraction of silicon (the molar silicon content divided by the sum of the molar carbon, oxygen, and silicon contents) was calculated based on the feed composition and the molecular structures. The variation of the tan δ peak temperature with the Si content for both nanocomposite polyHIPE systems is seen in Figure 11. Both V-40 (around 4 at % Si) and D-26 (0% Si) have tan δ peak temperatures of around −20 °C. The presence of unreacted VSQ vinyl groups in the polyHIPE, observed in the FTIR analysis, indicates that, on a molar basis, VSQ is less effective

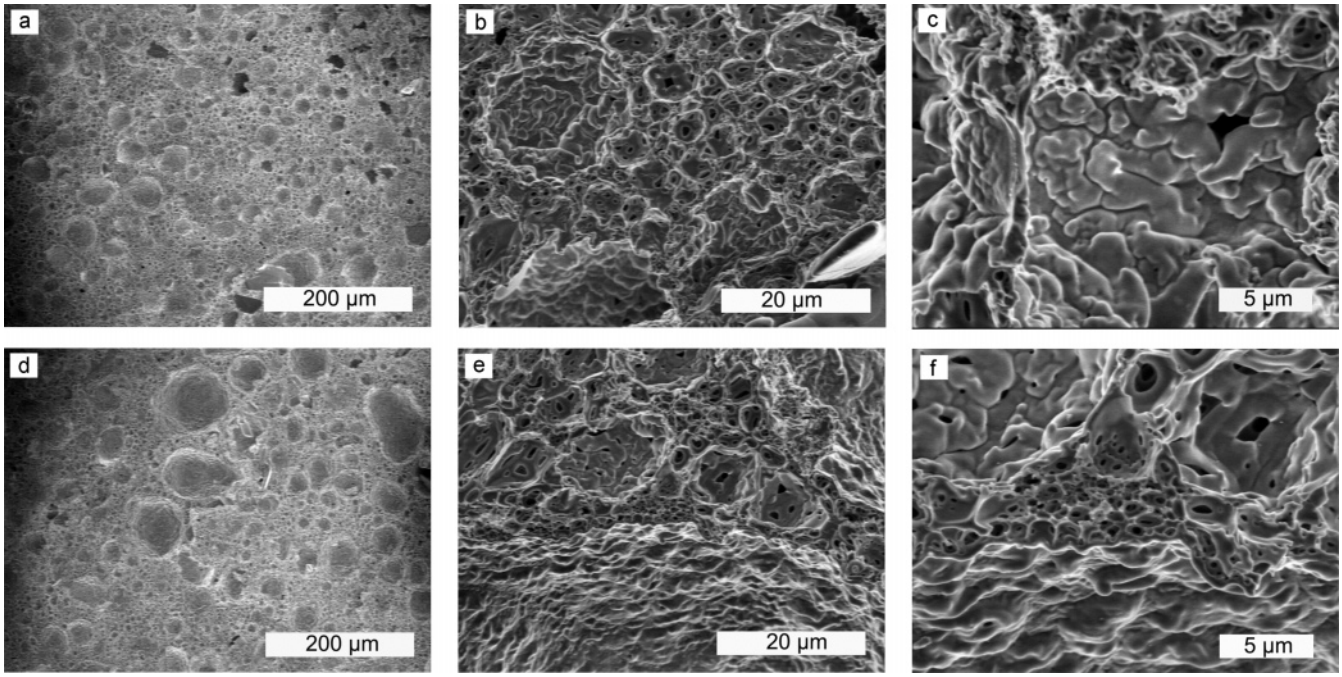

Figure 15. SEM micrographs of the porous inorganic monoliths: (a−c) V-40 and (d−f) V-50.

at cross-linking than DVB, for which unreacted vinyl groups were not observed. The similar tan δ peak temperature for 40 mol % VSQ and 26 mol % DVB confirms the relative effectiveness of DVB. It is interesting to note that the tan δ peak temperature increases with the Si content in a linear fashion for both polyHIPE systems and that the slopes of the lines are quite similar. This seems to indicate that the effects of the silica content are similar for both polyHIPE systems. However, owing to the presence of DVB in the POSS-containing polyHIPE, the tan δ peak temperatures for similar Si contents are quite different. Both V-40 and the POSS-containing polyHIPE with 9 mol % POSS (termed C-9) have around 4 atom % Si. However, V-40 has a tan δ peak temperature of −20 °C, while C-9 (the corresponding POSS-containing polyHIPE) has a tan δ peak temperature of 30 °C.

The variation of E' with temperature for C-9 (the POSS-containing polyHIPE with the same Si content as V-40) is also seen in Figure 8. As seen for the VSQ-containing polyHIPE, below their T_gs the polymers are glassy and exhibit similar E' plateaus. There are, however, significant differences in the E' rubbery plateaus above the T_gs. The E' rubbery plateau for C-9 is significantly larger than that for V-40. This significant increase in the E' rubbery plateau indicates that the EHA is stiffened to a greater extent by the combination of DVB and POSS.

A comparison in terms of Si content of the moduli from the stress−strain curves of VSQ-containing and POSS-containing polyHIPE is seen in Figure 12. The modulus is affected by many factors including, most prominently, the stiffness of the wall material (polymer backbone, degree of cross-linking, amount of reinforcement), the ratio of polyHIPE density to wall density, and the porous structure. The 0.58 MPa modulus of D-26 is almost an order of magnitude larger than the 0.06 MPa modulus of V-40. These results again demonstrate the effectiveness of DVB cross-linking versus VSQ cross-linking (the differences in polyHIPE density and porous structure are, in comparison, not as significant). All the POSS-containing polyHIPE with tan δ peak temperatures below room temperature (Figure 11) have moduli of around 0.6 MPa, similar to that of V-61. The modulus of C-9 (9 mol % POSS, around 4 at % Si), however, is 1.9 MPa. This modulus is more than an order of magnitude larger than the modulus of the corresponding VSQ-containing polyHIPE, V-40. This difference in moduli reflects the difference in the tan δ peak temperatures. V-40 has a tan δ peak temperature of −20 °C and is, therefore, relatively rubbery at room temperature. The corresponding POSS-containing polyHIPE has a tan δ peak temperature of 30 °C and is, therefore, relatively glassy at room temperature. This difference in the properties of the wall material yields the significant difference in moduli.

Porous Inorganic Monoliths. Previous investigations have shown that the pyrolysis of nanocomposite polyHIPE can yield porous inorganic monoliths (PIM).[7,40] Degradation of the VSQ-containing nanocomposite polyHIPE is described by the TGA and DTG thermograms in Figures 13 and 14, respectively. The two-stage degradation of D-26 has been described previously and is summarized in Table 4.[40] Briefly, D-26 has a T_d (temperature at which the mass loss is 10%) at 281 °C and exhibits two DTG peaks (285 and 344 °C) and a DTG shoulder (360 °C). As seen in Figures 13 and 14 and Table 4, the mass loss begins at significantly lower temperatures for V-40, with a T_d of 236 °C and a DTG peak at 241 °C. Degradation of V-50 is similar to that of V-40 but occurs at slightly higher temperatures and with a somewhat smaller mass loss. The first degradation stage is represented by a narrow DTG peak in D-26, V-40, and V-50. This peak occurs at lower temperatures for the nanocomposite polyHIPE than for D-26. In the second stage D-26 exhibits a rapid mass loss and a narrow DTG peak at 344 °C. The nanocomposite polyHIPE exhibit broad DTG peaks at similar temperatures that correspond to a significantly smaller and significantly more gradual mass loss.

Interestingly, pyrolysis of the VSQ-containing nanocomposite polyHIPE yields porous inorganic monoliths. The porous

Table 4. Thermal Degradation Results

	D-26	V-40	V-50
DTG peaks, °C	285	241	251
	344 (360)	342	361
T_d, °C	281	236	241
monolith density, kg/m^3		2.1×10^2	2.5×10^2

structures of the PIM based on V-40 and V-50 are seen in the SEM micrographs in Figure 15. These porous structures are quite similar to those of the corresponding polyHIPE in Figure 3. XPS reveals that the inorganic monoliths consist of a Si−O structure with an O/Si atomic ratio of 1.7 and 8.6 atom % C (33.6 atom % Si and 58.0 atom % O). The FTIR spectrum of the PIM based on V-50 in Figure 4 exhibits only traces of the organic groups seen in the spectra of the original polyHIPE. The band at 801 cm^{-1} is associated with Si−O−C, carbonaceous residue that is attached to the Si−O network structure. The FTIR spectrum from the VSQ-containing PIM is quite similar to that from the POSS-containing PIM.[40] The densities of the PIM from the VSQ-containing polyHIPE are around 2.3×10^2 kg/m^3, and the estimated porosities, assuming a density of 2.4×10^3 kg/m^3 for the Si−O network, are around 90%, similar to those of the original polyHIPE.

Conclusions

Novel silsesquioxane-cross-linked porous nanocomposites with densities of around 1.5×10^2 kg/m^3 were successfully synthesized within a HIPE. Destabilization of the HIPE/polyHIPE increased with increasing VSQ content, and it was difficult to discern a typical polyHIPE structure at high VSQ contents. The tan δ peak temperature, tan δ fwhm, room-temperature modulus, and stress at 40% strain all increased in a linear fashion with increasing VSQ content, reflecting the increase in cross-linking through reaction with the reinforcing Si−O network. On a molar basis, cross-linking with DVB produced higher tan δ peak temperatures and moduli than cross-linking with VSQ. This, in part, reflects the presence of unreacted VSQ vinyl groups and the absence of unreacted DVB vinyl groups. The influence of the Si content on the tan δ peak temperature was similar for both the VSQ-containing and POSS-containing polyHIPE. However, the POSS-containing polyHIPE had significantly higher tan δ peak temperatures and moduli for similar Si contents. Pyrolysis of the VSQ-containing polyHIPE yielded inorganic Si−O monoliths whose porous structures resembled those of the original polyHIPE.

Acknowledgment. The partial support of the Technion VPR fund is gratefully acknowledged.

References and Notes

(1) Cameron, N. R.; Sherrington, D. C. *J. Mater. Chem.* **1997**, *7*, 2209.
(2) Cameron, N. R. *Polymer* **2005**, *46*, 1439.
(3) Cameron, N. R.; Sherrington, D. C.; Albiston, L.; Gregory, D. P. *Colloid Polym. Sci.* **1996**, *274*, 592.
(4) Sergienko, A. Y.; Tai, H.; Narkis M.; Silverstein, M. S. *J. Appl. Polym. Sci.* **2004**, *94*, 2233.
(5) Sergienko, A. Y.; Tai, H.; Narkis, M.; Silverstein, M. S. *J. Appl. Polym. Sci.* **2002**, *84*, 2018.
(6) Tai, H.; Sergienko, A.; Silverstein, M. S. *Polym. Eng. Sci*. **2001**, *41*, 1540.
(7) Silverstein, M. S.; Tai, H.; Sergienko, A.; Lumelsky, Y.; Pavlovsky, S. *Polymer* **2005**, *46*, 6682.
(8) Desforges, A.; Backov, R.; Deleuze, H.; Mondain-Monval, O. *Adv. Funct. Mater.* **2005**, *15*, 1689.
(9) Katsoyiannis, I. A.; Zouboulis, A. I. *Water Res.* **2002**, *36*, 5141.
(10) Brown, I. J.; Clift, D.; Sotiropoulos, S. *Mater. Res. Bull.* **1999**, *34*, 1055.
(11) Sotiropoulos, S.; Brown, I. J.; Akay, G.; Lester, E. *Mater. Lett.* **1998**, *35*, 383.
(12) Livshin, S.; Silverstein, M. S. *Macromolecules* **2007**, *40*, 6349.
(13) Butler, R.; Davies C. M.; Cooper, A. I. *Adv. Mater.* **2001**, *13*, 1459.
(14) Butler, R.; Hopkinson I.; Cooper, A. I. *J. Am. Chem. Soc.* **2003**, *125*, 14473.
(15) Kulyagin, O.; Silverstein, M. S. Porous Poly(2-hydroxyethyl acrylate) Hydrogels Synthesized within High Internal Phase Emulsions. *Soft Matter* [Online early access]. DOI: 10.1039/b711610a.
(16) Normatov, J.; Silverstein, M. S. *Polymer* **2007**, *48*, 6648.
(17) Menner, A.; Haibach, K.; Powell, R.; Bismarck, A. *Polymer* **2006**, *47*, 7628.
(18) Menner, A.; Powell, R.; Bismarck, A. *Soft Matter* **2006**, *4*, 337.
(19) Haibach, K.; Menner, A.; Powell, R.; Bismarck, A. *Polymer* **2006**, *47*, 4513.
(20) Zhang, H.; Hardy, G. C.; Khimyak, Y. Z.; Rosseinsky, M. J.; Cooper, A. I. *Chem. Mater*. **2004**, *16*, 4245.
(21) Krajnc, P.; Leber, N.; Brown, J. F.; Cameron, N. R. *React. Funct. Polym.* **2006**, *66*, 81.
(22) Krajnc, P.; Stefanec, D.; Brown, J. F.; Cameron, N. R. *J. Polym. Sci., Part A: Polym. Chem.* **2005**, *43*, 296.
(23) Krajnc, P.; Leber, N.; Stefanec, D.; Kontrec, S.; Podgornik, A. *J. Chromatogr., A* **2005**, *1065*, 69.
(24) Akay, G.; Erhan, E.; Keskinler, B. *Biotechnol. Bioeng.* **2005**, *90*, 180.
(25) Erhan, E.; Yer, E.; Akay, G.; Keskinler, B.; Keskinler, D. *J. Chem. Technol. Biotechnol.* **2004**, *79*, 195.
(26) Moine, L.; Deleuze, H.; Maillard, B. *Tetrahedron Lett.* **2003**, *44*, 7813.
(27) Deleuze, H.; Maillard, B.; Mondain-Monval, O. *Bioorg. Med. Chem. Lett.* **2002**, *12*, 1877.
(28) Baney, R. H.; Itoh, M.; Sakakibara, A.; Suzuki, T. *Chem. Rev*. **1995**, *95*, 1409.
(29) Liu, H.; Zheng, S. *Macromol. Rapid Commun.* **2005**, *26*, 196.
(30) Pittman, C. U., Jr.; Li, G.-Z.; Ni, H. *Macromol. Symp.* **2003**, *196*, 301.
(31) Lu, T.; Liang, G.; Guo, Z. *J. Appl. Polym. Sci.* **2006**, *101*, 3652.
(32) Liu, Y.; Meng, F.; Zheng, S. *Macromolecules* **2005**, *26*, 920.
(33) Yang, C.-C.; Chen,W.-C.; Chen, L.-M.; Wang, C.-J. *Proc. Natl. Sci. Counc. ROC(A)* **2005**, *25*, 339.
(34) Cha, B. J.; Yang, J. M. *J. Appl. Polym. Sci.* **2007**, *104*, 2906.
(35) Silverstein, M. S.; Shach-Caplan, M.; Khristosov, M.; Harel, T. Effects of Plasma Exposure on SiCOH and MSQ Films. *Plasma Processes Polym.* [Online early access]. DOI: 10.1002/ppap.200700079.
(36) Amir, N.; Levina, A.; Silverstein, M. S. *J. Polym. Sci. A: Polym. Chem.* **2007**, *45*, 4264.
(37) Tai, H.; Sergienko, A.; Silverstein, M. S. *Polymer* **2001**, *42*, 4473.
(38) Sluzney, A.; Silverstein, M. S.; Kababya, S.; Schmidt A.; Narkis, M. *J. Polym. Sci.: Polym. Chem.* **2001**, *39*, 8.
(39) Sluszny, A.; Silverstein, M. S.; Narkis N.; Narkis, M. *J. Appl. Polym. Sci.* **2001**, *81*, 1429.
(40) Normatov, J.; Silverstein, M. S. Porous Polymer-POSS Nanocomposites Synthesized within High Internal Phase Emulsions. Submitted for publication.
(41) Barbetta, A.; Cameron, N. R. *Macromolecules* **2004**, *37*, 3188.
(42) Barbetta, A.; Cameron, N. R. *Macromolecules* **2004**, *37*, 3202.
(43) Colthup, N. B; Daly, L. H. *Introduction to infrared and Raman spectroscopy*, 3rd ed.; Academic Press: New York, 1990.
(44) Liu, L.; Hu, Y.; Song, L. *High Perform. Polym.* **2006**, *18*, 919.

MA071417T